Inorganica Chimica Acta, 58 (1982) 179–185
© Elsevier Sequoia S.A., Lausanne – Printed in Switzerland

Carbon Monoxide and Isocyanide Binding to Iron(II) Complexes of Tetradentate Bis Di-Imine and Bis Di-Oxime and Mixed Oxime-Imine Macrocycles

DENNIS V. STYNES*, KOWSILL SINGH, BETTY NG and SUSAN WILSHIRE

Department of Chemistry, York University, 4700 Keele Street, Downsview, Ont., Canada

Received June 15, 1981

The synthesis and characterization of new low spin Fe(II) complexes of diacetylmonoximeiminodiacetylmonoximato-1,3 propane (DOHpn), and ethane (DOHen), and of 2,3,9,10 tetramethyl 1,4,8,11 tetra-azacyclotetradeca 1,3,8,10 tetraene (TIM) are reported; $[Fe(N_4)(CH_3Im)X](PF_6)_2$ *X* = CH_3Im, *CO, and benzylisocyanide (BZNC). Kinetic studies for CO and BZNC dissociation are compared with corresponding data for analogous* FeN_4 *systems. The relative lability of CO is DMGH < DOHpn < DOHen < TIM, TAAB, 14-ane < Porphyrin, Phthalocyanine < 15-ane.* Trans *effects of CO and BZNC are discussed.*

Introduction

Studies of carbon monoxide and isocyanide binding to a wide range of tetragonal iron(II) complexes (FeN_4L_2) containing the tetradentate planar macrocyclic ligands N_4 = porphyrin (P) [1–3], phthalocyanine (Pc) [3–5], bisdimethylglyoxime $(DMGH)_2$ [6, 7], TAAB [8], 14-ane, and 15-ane [9, 10], have been reported. These systems differ in ring size, degree of unsaturation, overall charge, ligand conformation, and flexibility, ligand field strength, and π-bonding. They all undergo axial ligand substitution reactions *via* a dissociative mechanism and the kinetics and equilibrium data span a range of over 10^6. In addition to the large *cis* effects of the tetradentate ligand N_4, some unusual *trans* effects are also observed [11].

Previous studies have dealt with neutral or dipositive complexes of Fe(II). We now report the synthesis and axial ligation studies of unipositively charged complexes of DOHpn and DOHen [12]. The DOH systems are of interest since they are structurally half-way between the bis-glyoxime system $(DMGH)_2$ and the tetraimine ligand TIM reported previously by Rose [13]. While cobalt complexes of DOH have been reported previously [14–16], apparently no report of iron complexes of these ligands have appeared. We also report data for the $FeTIM^{+2}$ system. Some photochemical [17, 18] and kinetic studies [9, 11, 19, 20] of Fe(II)TIM have been reported previously.

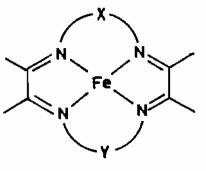

X = Y = O–H–O $Fe(DMGH)_2$
X = $(CH_2)_3$ Y = O–H–O $[FeDOHpn]^+$
X = $(CH_2)_2$ Y = O–H–O $[FeDOHen]^+$
X = Y = $(CH_2)_3$ $[FeTIM]^{+2}$

Experimental

Ferrous acetate was prepared from iron powder and glacial acetic acid and stored under nitrogen. The ligands DOH_2en and DOH_2pn were prepared from butanedionemonoxime and ethylenediamine or propanediamine by the method of Uhlig [12] $[FeTIM(CH_3CN)_2](PF_6)_2$, $[FeTIM(CH_3CN)(CO)](PF_6)_2$, and $[FeTIM(CH_3Im)_2](PF_6)_2$ were prepared by the method of Rose [13].

$[Fe(DOHpn)(CH_3Im)_2]PF_6$

Ferrous acetate (2.5 g) and DOH_2pn (3.0 g) were dissolved in a degassed mixture of 25 ml CH_3CN and 5 ml CH_3IM under nitrogen in double-arm Schlenk tube equipped with a frit giving a deep blue solution. The solution was filtered under nitrogen and a degassed solution of 5 g NH_4PF_6 in 15 ml CH_3CN added to the filtrate. After standing at 0 °C overnight, a blue precipitate was obtained. This was filtered and washed with ether to give 8.2 g of crude product.

---

*Author to whom correspondence should be addressed.

****Abbreviations**: DMGH dimethylglyoximate; DOHpn diacetylmonoximeiminodiacetylmonoximato-1,3-propane; DOHen diacetylmonoximeiminodiacetylmonoximato-ethane; TIM 2,3,9,10-tetramethyl-1,4,8,11-tetra-azacyclotetradeca-1,3,8,10-tetraene; TAAB tetrabenzo (b, f, j, n) (1,5,9,13) tetra-azacyclohexadecine; Pc phthalocyanine; CH_3Im 1-methyl imidazole; BZNC benzylisocyanide; 14-ane-1,4,8,11-tetra-azacyclotetradecane; 15-ane-1,4,8,11-tetra-azacyclopentadecane; P-protoporphyrin IX: TPP-tetraphenylporphyrin.

TABLE I. Analytical Data.

Complex		C	H	N
$[Fe(DOHpn)(CH_3Im)_2]PF_6$	Calcd.	37.76	5.17	18.54
	Found	37.45	5.06	18.25
$[Fe(DOHpn)(CH_3Im)(CO)]PF_6 \cdot CH_2Cl_2$	Calcd.	32.15	4.28	13.23
	Found	32.19	4.12	13.61
$[Fe(DOHpn)(CH_3Im)(BZNC)]PF_6$	Calcd.	43.20	5.04	15.33
	Found	42.86	4.79	15.36
$[FeTIM(CH_3Im)(BZNC)](PF_6)_2$	Calcd.	39.36	4.70	12.36
	Found	39.30	4.43	12.26
$[FeTIM(BZNC)_2](PF_6)_2$	Calcd.	43.49	4.62	10.14
	Found	43.22	4.74	10.33

TABLE II. Comparative Spectral Data for FeN_4XY Complexes.

X	Y	$Fe(TIM)^{+2}$	$Fe(DOHpn)^+$	$Fe(DOHen)^+$	$Fe(DMGH)_2$
Visible Spectra λmax (nm)					
CH_3Im	CH_3Im	667	602	580	531
CH_3Im	CO	450	418	416	385
CH_3Im	BZNC	555	500	490	445
$BZNC_2$	BZNC	490	440	450	392
Infra-red ν_{nc} or ν_{co}					
CH_3Im	CO	2030	1993	2026	1978
CH_3Im	BZNC	2181	2151	2145	2141
BZNC	BZNC	2189	–	–	2167
Chemical shift of CH_3 resonance (ppm)					
CH_3Im	CH_3Im	2.80	2.66, 2.60	2.64, 2.51	
CH_3Im	CO	2.45	2.38, 2.27	2.39, 2.30	2.14
CH_3Im	BZNC	2.53	2.35, 2.29	2.39, 2.33	2.16

A white impurity was removed by dissolving 1 g of crude product in 40 ml CH_2Cl_2, filtering, and concentrating the filtrate to give 0.4 g of pure material. NMR ($CDCl_3/CD_3CN$) DOHpn δ 2.66, 2.60 (12H), 4.0 (4H), CH_3Im 3.55 (6H), 6.00 (2H), 6.53 (2H), 6.63 (2H).

$[Fe(DOHpn)(CH_3Im)(CO)]PF_6 \cdot CH_2Cl_2$

Carbon monoxide was bubbled through a solution of 1 g $[Fe(DOHpn)(CH_3Im)_2PF_6$ in 125 ml CH_2Cl_2. The solution turned from blue to yellow–green over a period of 1 hour. Ether was added and the solution cooled while maintaining CO bubbling and then left in the freezer overnight giving yellow–green crystals. These were filtered in air and washed with ether. Yield 0.3 g NMR: ($CDCl_3\delta$ DOHpn 2.38, 2.27 (12H), 3.95 (4H), CH_3Im 3.70 (3H), 6.58 (1H), 6.81 (1H), 7.25 (1H), CH_2Cl_2 5.27 (2H).

$[Fe(DOHpn)(CH_3Im)(BZNC)]PF_6$

$[Fe(DOHpn)(CH_3Im)_2]PF_6$ (0.5 g) was added to a solution of 0.15 g BZNC in 20 ml methanol under nitrogen and stirred for 10 minutes. The solution was cooled and 30 ml ether added. A resulting brown solid was filtered, washed with ether and dried *in vacuo.* Yield 0.3 g. NMR: (CD_3CN)δ DOHpn 2.35, 2.29 (12H), 3.82 (4H), CH_3Im 3.59 (3H), 6.29 (1H), 6.92 (2H), BZNC 1.96 (2H), 7.35 (5H).

$[Fe(DOHpn)(BZNC)_2]PF_6$

A solution of $[Fe(DOHpn)(CH_3Im)(BZNC)]PF_6$ was heated at 60 °C in a thermostatted 1 cm path length cell, initial A = 1.5 at 500 nm in methylethyl ketone with 0.05 g BZNC. The absorbance at 500 nm decreased and a new peak grew in at 440 nm assigned to the bis isocyanide complex ($t_{1/2}$ = 6 hrs at 60 °C). The Fe(DOHen) analogs were prepared by similar methods.

[FeTIM(BZNC)$_2$](PF$_6$)$_2$

BZNC (0.2 g) was added to a solution at 0.4 g [Fe(TIM)(CH_3CN)$_2$]PF_6 in 5 ml acetonitrile and the solution maintained at 50 °C for 1 hour. The resulting yellow solution (λmax = 490 nm) was cooled and ethanol added to induce precipitation. The orange precipitate was filtered, washed with ethanol and ether and dried *in vacuo*. Yield 0.4 g NMR (CD_3CN) δ TIM 2.35 (12H), 3.81 (8H), BZNC 4.82 (4H), 7.3 (10H).

[Fe(TIM)(CH$_3$Im)(BZNC)](PF$_6$)$_2$

BZNC (0.08 g) was added to a solution of [Fe-TIM(CH_3Im)$_2$](PF_6)$_2$ in 4 ml CH_3CN giving an immediate color change from blue to red. Ethanol was added and the precipitate filtered, washed with ethanol and dried *in vacuo*. Yield 0.2 g. NMR (CD_3-CN) δ TIM 2.53 (12H), 3.81 (8H), CH_3Im 3.60 (3H), 5.94 (1H), 6.59 (1H), 6.97 (1H), BZNC 4.75 (2H), 7.3 (5H).

Kinetic Measurements

Kinetic studies were carried out as described previously [5] and pseudo-first order rate constants derived by standard methods. Log plots were linear over 3 half lives and analysis at λmax of the product or reactant were typically within experimental error. In the case of the reaction FeTIM(CH_3Im)(BZNC)$^{+2}$ + CH_3Im carried out in neat CH_3Im a slow decomposition of the product interfered with analysis of the data at 665 nm. Analysis at 555 nm gave linear log plots over 3 half lives which were in agreement with analysis at 665 nm for the first half-live prior to appreciable decomposition. A similar decomposition is even more pronounced in the Fe(DOHen) system. Only a slight decomposition is observed in the Fe-(DOHpn) system for this reaction. Reactions of the carbonyl complexes carried out under milder conditions show no evidence for any side reactions.

Results

Spectral Data: The CH_3Im, CO, and BZNC complexes of the FeDOHpn$^+$ display spectroscopic properties intermediate between those of Fe(DMGH)$_2$ and FeTIM^{+2} derivatives (Table II). The visible spectra are assigned to charge transfer transitions from metal to π orbitals of the unsaturated ligand system. The systematic shift to shorter wavelength (about 50 nm per unit of charge) is consistent with the expected greater ease of oxidation of iron as the charge on the complex is reduced. Consistent with this are qualitative observations on the air sensitivity of the $FeN_4(CH_3Im)_2$ complexes. The TIM complex is air-stable, the DOH complexes somewhat air sensitive and the DMGH complex very air sensitive in solution (all of the complexes are reasonably air stable in the solid state when dry). The ν_{co} and ν_{nc} show that π back bonding to CO and BZNC decreases as the charge increases in this systematic series of complexes. The NMR of the DOH complexes show nonequivalent resonances for the methyls adjacent to the oxime and imine groups which are between the corresponding positions for TIM and (DMGH)$_2$ complexes.

Kinetics

Previous kinetic studies of a wide range of FeN_4XY complexes have shown a dissociative mechanism (D) for axial ligand substitution reactions.

$$FeN_4XY \underset{k_{+y}}{\overset{k_{-y}}{\rightleftharpoons}} FeN_4X \underset{k_{-x}}{\overset{k_{+x}}{\rightleftharpoons}} FeN_4X_2$$

The pseudo-first order rate constant, neglecting the reverse reaction is given by:

$$k_{obs} = \frac{k_{-y}k_{+x}[X]}{k_{+x}[X] + k_{+y}[Y]}$$

In this study, all reactions were carried out with a large excess of entering ligand [X] and negligible [Y]. Under these conditions the above expression reduces to $k_{obs} = k_{-y}$, *i.e.* the pseudo-first order rate constant corresponds to the rate constant for dissociation of Y. The kinetics of reactions:

$$FeN_4(CH_3Im)_2 + X \rightarrow FeN_4(CH_3Im)(X) + CH_3Im$$

X = CO, BZNC N_4 = TIM, DOHen, DOHpn

are too fast to measure using conventional spectrophotometric methods at room temperature. A NMR study of CH_3Im exchange in FeTIM(CH_3Im)$_2^{+2}$ gives k_{-CH_3Im} = 0.45 at 25 °C [19]. A stopped-flow study of FeTIM(CH_3CN)$_2^{+2}$ gives k_{-CH_3CN} = 195 s^{-1} at 30 °C [20].

The reversible binding of CO to FeTIM(CH_3CN)$_2^{+2}$ in CH_3CN solution was previously described by Rose [13]. Kinetic data for the reactions:

$$FeTIM(CH_3CN)(CO)^{+2} + CH_3CN \rightarrow FeTIM(CH_3CN)_2^{+2} + CO$$

were conveniently measured in acetonitrile solution. The corresponding reaction of the FeTIM(CH_3Im)$_2^{+2}$ complex with CO in acetonitrile is complicated by solvent coordination. Thus dilution of blue aceto-

TABLE III. Kinetic Data for CO Dissociation from FeN_4LCO Complexes.

	k_{-co} s^{-1} (25 °C)	$\Delta H^{\ddagger}$ kcal/mole	$\Delta S^{\ddagger}$ eu	
$Fe(DMGH)_2(CH_3Im)(CO)$	3.1×10^{-6} [a]	27	6	ref. 7
$Fe(DOHpn)(CH_3Im)(CO)^+$	1×10^{-4} [b]	25.8[f]	9	this work
$Fe(DOHen)(CH_3Im)(CO)^+$	2.4×10^{-4} [b]	23.7[g]	4	this work
$FeTIM(CH_3Im)(CO)^{+2}$	1.2×10^{-3} [c]			this work
$FeTIM(CH_3CN)(CO)^{+2}$	4.3×10^{-4} [b]	24.3[h]	7.5	this work
$FeTAAB(CH_3Im)(CO)^{+2}$	6.5×10^{-3} [c]			ref. 8
$FePc(CH_3Im)(CO)$	2×10^{-2} [d]	24	10	ref. 4
$FeP(Im)(CO)$	0.8×10^{-2} [e]	25	15	ref. 31, 32
$Fe(14ane)(CH_3CN)(CO)^{+2}$	7.7×10^{-4} [b]			ref. 9
$Fe(15ane)(CH_3CN)(CO)^{+2}$	1.7[b]	19.2	7	ref. 9

[a] Neat CH_3Im. [b] CH_3CN. [c] Acetone. [d] Toluene. [e] For chelated protoheme in aqueous cetyltrimethylammonium bromide suspension. k_{-co} is 2.8×10^{-2} s^{-1} for deuteroheme dme in benzene at 20 °C [30]. [f] Temperature dependence of k_{-co}: 30 °C, 2.0×10^{-4}; 40 °C, 8.3×10^{-4}; 50 °C, 3.0×10^{-3}; 60 °C. 1.0×10^{-2} s^{-1}. [g] Temperature dependence of k_{-co}: 30 °C, 5.5×10^{-4}; 40 °C, 1.8×10^{-3}; 50 °C, 6.1×10^{-3} s^{-1}. [h] Temperature dependence of k_{-co}: 35 °C, 1.7×10^{-4}; 40 °C, 3.3×10^{-3}; 45 °C, 5.9×10^{-3} s^{-1}.

nitrile solutions of $FeTIM(CH_3Im)_2^{+2}$ (λmax 667) results in the decrease in the 667 nm band and the growth of new peaks at ~605 and 550 assigned to $FeTIM(CH_3Im)(CH_3CN)^{+2}$ and $FeTIM(CH_3CN)_2^{+2}$ respectively. In the presence of CO, a yellow solution is observed which may have either CH_3Im or CH_3CN *trans* to CO. The situation is less complicated in acetone solution which does not compete as effectively with CH_3Im as a ligand [20]. Addition of CO to $FeTIM(CH_3Im)_2^{+2}$ in acetone gives a color change from blue to yellow-green with the appearance of a peak at 450 nm. In contrast, $FeTIM(CH_3CN)(CO)^{+2}$ dissolved in acetone gives a peak at 428 nm. Addition of CH_3Im to this solution results in a rapid reaction ($k = 2 \times 10^{-2}$ s^{-1} at 25 °C independent of $[CH_3Im]$) resulting in the disappearance of the 428 nm band and the growth of the 450 nm band. We assign these spectral changes to the reaction $FeTIM(CH_3CN)(CO)^{+2} + CH_3Im \rightarrow FeTIM(CH_3Im)(CO)^{+2} + CH_3CN$. Following these spectral changes, a slower reaction to give $FeTIM(CH_3Im)_2^{+2}$ λmax 665 nm $k = 1.2 \times 10^{-3}$ s^{-1} is observed. A similar replacement of acetonitrile *trans* to BZNC in $FeTIM(CH_3CN)(BZNC)^{+2}$ in acetone is observed. Addition of CH_3Im to an acetone solution of $FeTIM(CH_3CN)(BZNC)^{+2}$ at 25 °C results in the disappearance of the 520 nm band of the starting complex and the formation of $FeTIM(CH_3Im)(BZNC)^{+2}$ λmax = 555 nm, $k_{obs} = 5 \times 10^{-3}$ s^{-1}. This rate is identical to that for the reaction of $FeTIM(CH_3CN)(BZNC)^{+2}$ with BZNC in acetone [9], confirming the independence of the rate on the nature of the entering ligand as expected for a D mechanism.

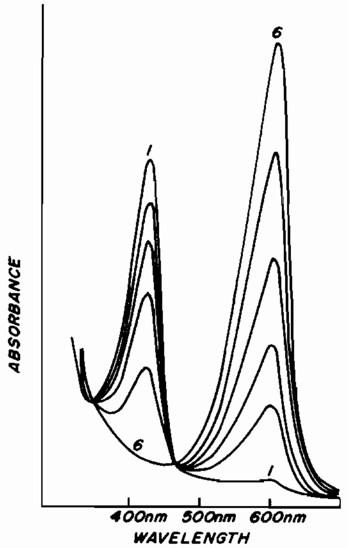

Fig. 1. Spectral changes with time for the reaction $Fe(DOHpn)(CH_3Im)(CO)^+ + CH_3Im \rightarrow Fe(DOHpn)(CH_3Im)_2^+ + CO$ in acetonitrile.

Corresponding replacement of CH_3Im *trans* to BZNC by acetonitrile occurs at a much slower rate. Dissolution of $FeTIM(CH_3Im)(BZNC)^{+2}$ in acetonitrile at 60 °C results in a clean first-order reaction to give the $FeTIM(CH_3CN)(BZNC)^{+2}$ complex (λmax = 520 nm) $k = 1.5 \times 10^{-3}$ s^{-1}.

Rate constants for the reactions:

$FeN_4(CH_3Im)(CO) + CH_3Im \rightarrow$

$FeN_4(CH_3Im)_2 + CO$ for N_4 = DOHen and DOHpn

TABLE IV. Kinetics of BZNC and CH_3Im Substitution in $FeN_4(CH_3Im)(BZNC)$ Complexes at 60 °C.

	$k^{CH_3Im}_{-BZNC}$ s^{-1}	$k^{BZNC}_{-CH_3Im}$ s^{-1}	
FeTIM	4×10^{-3} [a]	1.5×10^{-3} [e]	this work
FeDOHpn	4×10^{-4} [a]	3×10^{-5} [f]	this work
$Fe(DMGH)_2$	4.6×10^{-4} (65 °C)[a]	2×10^{-5} [g]	ref. 7
FeTAAB	5.6×10^{-3} [b]	1.28×10^{-2} [f]	ref. 8
FePc	8.2×10^{-3} [c]	2.9×10^{-2} (30 °C)[g]	ref. 5
FeP	0.5 (20 °C)[d]	–	ref. 1

[a] Replacement by CH_3Im in neat CH_3Im. [b] Replacement by CH_3Im in butanone. [c] Replacement by CH_3Im in toluene. [d] For BUNC on chelated protoheme, in benzene. [e] Replacement by CH_3CN in acetonitrile. [f] Replacement by BZNC in butanone. [g] Replacement by BZNC in toluene.

were conveniently measured in acetonitrile solution containing 0.1 to 1 *M* CH_3Im. Typical spectral changes are shown in Fig. 1. The high concentration of excess CH_3Im prevents CH_3CN coordination.

Reactions of the isocyanide complexes were substantially slower. The reaction:

$$FeN_4(CH_3Im)(BZNC) + CH_3Im \rightarrow FeN_4(CH_3Im)_2 + BZNC$$

was carried out in neat CH_3Im at elevated temperatures. The lability of CH_3Im *trans* to BZNC was studied in the reaction:

$$Fe(DOHpn)(CH_3Im)(BZNC) + BZNC \rightarrow FeN_4(BZNC)_2 + CH_3Im$$

The observed rate constant in butanone is 3×10^{-5} s^{-1}. The substantially greater inertness of CH_3Im when *trans* to BZNC is similar to effects previously described for $N_4 = (DMGH)_2$ [7] and TAAB [8].

Kinetic data for the DOHpn, DOHen, and TIM systems are given in Tables III and IV along with corresponding results for analogous FeN_4 systems.

Discussion

The spectral and kinetic data for the $Fe(DMGH)_2$, $FeDOHpn^+$, and $FeTIM^{+2}$ complexes demonstrate a systematic variation in properties with variation in structure. The increased net positive charge on the complex resulting from substitution of an imine for an oxime group in the macrocyclic ligand results in increased lability for π-acceptor ligands CO and BZNC. These systems may be compared with a variety of analogous FeN_4 systems including neutral, unipositive, and dipositively charged complexes, both saturated and unsaturated ring systems, and macrocycles differing in ring size including 13 (DOHen), 14 (DMGH, DOHpn, TIM, 14ane), 15 (15ane), and 16 (Pc, P, TAAB) membered rings.

CO Complexes

Data for CO dissociation are given in Table III. All of the systems listed undergo substitution via a dissociative mechanism. The rates, where studied as a function of solvent are typically insensitive to solvent variations as is expected for dissociation of a neutral CO ligand. The effect of the *trans* ligand is typically also rather small in comparison with the large *cis* effects.

The dipositive complexes of TIM, TAAB, and 14-ane give remarkably similar CO dissociation rates in spite of large differences in the macrocycle ring size and unsaturation. Only in the 15-ane complex is the CO dissociation rate significantly greater. The greater lability of the 15-ane system has previously been discussed [9] in terms of the mismatch of the 15-ane ring (ideal M–N distance of 2.28 Å [21] compares with strain free Fe–N distances of 1.98 and 2.18 Å for low and high spin complexes of α picolylamine [22]. Both the 14-ane and TAAB rings would seem to be too large for a low spin Fe^{+2}, however, they are able to accommodate a low spin Fe^{+2} without incurring significant conformational strain. This is achieved by puckering of the macrocycle. The flexibility of the TAAB ligand is shown in X-ray structures of low and high spin Ni^{+2} complexes with Ni–N distances of 1.90 and 2.10 Å respectively [23].

The DOHpn and DOHen systems provide another test of the effect of ring size on axial ligation to iron. The $Fe(DOHen)(CH_3Im)(CO)^+$ complex is only a factor of 2 more labile than the corresponding DOHpn derivative. The O–H–O unit is probably more flexible and not rigorously comparable to a $(CH_2)_3$ unit [24]. The greater lability of the DOHen derivative correlates with qualitative observations that the DOHen ligand is somewhat strained in fitting around an Fe^{+2}. DOHen is reported to be a poorer ligand than DOHpn in nickel complexes [14].

BZNC Complexes

The corresponding kinetic data for BZNC replacement *trans* to CH_3Im (Table IV) show effects similar to those observed in the CO complexes. The relative lability of BZNC is $(DMGH)_2 < DOHpn < TIM < Pc < P$. The DOHen system gives a $k^{CH_3Im}_{-BZNC}$ of 7×10^{-4} s^{-1} at 60 °C, about a factor of 2 faster than the DOHpn complex.

Trans *Effects*

The rates of CH_3Im replacement *trans* to BZNC are also given in Table IV. For FeDOHpn and $FeTIM^{+2}$ the lability of CH_3Im *trans* to BZNC is at least 1000 fold less than in the $FeN_4(CH_3Im)_2$ complexes. This large *trans* delabilizing effect of BZNC has been observed previously in $Fe(DMGH)_2$ and $Fe(TAAB)^{+2}$ complexes. These large *trans* effects of BZNC are remarkable, especially since equally dramatic *trans* effects in the opposite direction are observed in ruthenium porphyrins [25, 26] and phthalocyanines [27]. In the ruthenium systems axial substitution in the $RuP(CH_3Im)_2$ or $RuPc(CH_3Im)_2$ complexes require prolonged refluxing at elevated temperatures while exchange of CH_3Im in $RuP(CH_3Im)(CO)$ and $RuP(CH_3Im)(BZNC)$ is rapid.

Both CO and BZNC exert similar *trans* delabilizing effects on CH_3CN in FeTIM complexes. The lability of CH_3CN at 25 °C in acetone solution in FeTIM complexes is 122 s^{-1} [28] 0.02 s^{-1}, and 0.005 s^{-1} *trans* to CH_3CN, CO, and BZNC respectively.

Carbon monoxide has previously been found to exert a delabilizing effect on imidazoles in heme carbonyl complexes. The rates of Im dissociation from hemes in benzene *trans* to Im and CO are 1500 s^{-1} and 2.6 s^{-1} respectively [29, 30]. The magnitude of the effect on Im lability in the heme system is comparable to that on CH_3CN in the $FeTIM^{+2}$ system.

The *trans* effects may depend on the spin state of the transition state. Strong field ligands like CO and BZNC give low spin 5 coordinate complexes in heme systems while weaker field ligands like imidazoles give high spin 5 coordinate complexes. Thus in the dissociation of a group *trans* to a weak field ligand, a spin change occurring along the reaction coordinate would assist dissociation. If a strong field ligand like CO or BZNC is present, the complex would remain low spin throughout the reaction coordinate for ligand dissociation and thus remain inert. The fact that a labilizing, rather than a delabilizing effect of CO and BZNC is found in ruthenium systems [25–27] would support this hypothesis since in no case would a spin change be expected in the ruthenium systems. Based on the *trans* effect of BZNC, we suggest that all of FeN_4 systems listed in Table IV have high spin FeN_4CH_3Im intermediates and low spin FeN_4BZNC intermediates with the exception of FePc. As noticed previously, the FePc system shows *trans* effects opposite to the other systems possibly indicating a low or intermediate spin $Fe(Pc)CH_3Im$ intermediate. This would account for the 10^6 difference in CH_3Im lability in $FePc(CH_3Im)_2$ and $FeTPP(CH_3Im)_2$. ($k^{CH_3Im}_{-CH_3Im} = 1.3 \times 10^{-3}$ s^{-1} and $k^{CH_3Im}_{-CH_3Im} = 1.5 \times 10^{+3}$ s^{-1^3} [31] respectively).

Acknowledgement

We thank the Natural Science and Engineering Research Council for financial support.

References

1 T. G. Traylor and D. V. Stynes, *J. Am. Chem. Soc., 102,* 5938 (1980).
2 C. J. Weschler, D. L. Anderson and F. Basolo, *J. Am. Chem. Soc., 97,* 6707 (1975).
3 D. V. Stynes, *J. Am. Chem. Soc., 96,* 5942 (1974).
4 D. V. Stynes and B. R. James, *J. Am. Chem. Soc., 96,* 2733 (1974).
5 D. V. Stynes, *Inorg. Chem., 16,* 1170 (1977).
6 L. Vaska and T. Yamaji, *J. Am. Chem. Soc., 93,* 6673 (1971).
7 I. W. Pang and D. V. Stynes, *Inorg. Chem., 16,* 590 (1977).
8 I. W. Pang and D. V. Stynes, *Inorg. Chem., 16,* 2192 (1977).
9 D. V. Stynes, Y. S. Hui and V. Chew, *Inorg. Chem.,* in press.
10 D. D. Watkins, D. P. Riley, J. A. Stone and D. H. Busch, *Inorg. Chem., 15,* 387 (1976).
11 I. W. Pang, K. Singh and D. V. Stynes, *J. Chem. Soc. Commun.,* 132 (1976).
12 E. Uhlig and M. Friedrich, *Z. Anorg. Allg. Chem., 343,* 299 (1966).
14 D. Baldwin, R. M. Pfeiffer, D. W. Reichgott and N. J. Rose, *J. Am. Chem. Soc., 95,* 5152 (1973).
14 G. Costa, G. Mestroni and E. de Savorgnani, *Inorg. Chim. Acta, 3,* 323 (1969).
15 R. J. Guschl and T. L. Brown, *Inorg. Chem., 13,* 959 (1974).
16 J. H. Espenson, H. L. Fritz, R. A. Heckman and C. Nicolini, *Inorg. Chem., 15,* 906 (1976).
17 M. J. Incorvia and J. Zink, *Inorg. Chem., 16,* 3161 (1977).
18 C. I. Irwin and D. V. Stynes, *Inorg. Chem., 17,* 2682 (1978).
19 C. E. Holloway, D. V. Stynes and C. P. J. Vuik, *J. Chem. Soc. Dalton,* 124 (1979).
20 D. Hamilton, T. J. Lewis and N. K. Kildahl, *Inorg. Chem., 18,* 3364 (1979).
21 L. Y. Martin, S. C. Jackels, A. M. Tait and D. H. Busch, *J. Am. Chem. Soc., 99,* 4029 (1977).
22 A. M. Greenway and E. Sinn, *J. Am. Chem. Soc., 100,* 8080 (1978).
23 S. W. Hawkinson and E. B. Fleischer, *Inorg. Chem., 8,* 2402 (1969).

24 S. Brückner, M. Calligaris, G. Nardin and L. Randaccio, *Inorg. Chim. Acta, 3,* 278 (1969).

25 C. E. Holloway, D. V. Stynes and C. P. J. Vuik, *J. Chem. Soc. Dalton,* in press.

26 S. S. Eaton and G. R. Eaton, *Inorg. Chem., 16,* 72 (1977).

27 F. Pomposo and D. V. Stynes, to be submitted.

28 Calculated from data in reference 20.

29 D. K. White, J. Cannon and T. G. Traylor, *J. Am. Chem. Soc., 101,* 2443 (1979).

30 D. Lavelette, C. Tetreau and M. Momenteau, *J. Am. Chem.., 101,* 5395 (1979).

31 T. G. Traylor and A. P. Berzinis, *Proc. Nat. Acad. Sci. U.S.A., 77,* 3171 (1980).

32 T. G. Traylor, D. Cambell, V. Sharma and J. Geibel, *J. Am. Chem. Soc., 101,* 5376 (1979).